International Journal of Environmental Sciences
ISSN: 2229-7359
Vol. 11 No. 21s, 2025
https://theaspd.com/index.php

Fabrication of Mos_2-Chitosan Nanocomposites for Environmental Remediation Applications

KS Pushpa Valli[1], S. Mary Jelastin Kala[1]
[1]Department of Chemistry, St. Xavier's College, Affiliated to Manonmaniam Sundaradanar University, Abishekapatti, Tirunelveli-12, Tamil Nadu, India. Email Address: pushpa1989daniel@gmail.com

Abstract
Accelerated industrial growth results in environmental contamination, particularly in aquatic ecosystems. Photocatalytic degradation is an efficient and environmentally sustainable method for addressing industrial pollution, as it may completely decompose various water pollutants into non-toxic forms. Chitosan (CS) and molybdenum disulfide (MoS_2) facilitate effective dye degradation; nevertheless, MoS_2 possesses certain drawbacks. This study therefore synthesised a MoS2 hybrid nanocomposite based on chitosan (CS) to address these issues by improving the degradation of dye molecules, particularly Methylene Blue (MB), under sun light. The synthesized MoS_2@CS hybrid nanocomposite was comprehensively analyzed utilizing many analytical techniques, including XRD, SEM, UV-Visible, and PL spectroscopy. Various affecting parameters, including irradiation duration, initial dye concentration initial pH and dosage, were improved using batch mode. The heterogeneous MoS_2@CS water hybrid nanocomposite might promote the photodegradation of MB. The attenuated band gap of MoS_2@CS renders it effective for the degradation of MB, achieving a maximum degradation capability of 95% after 90 mins at pH 8 with a minimal dosage of 50 mg. A potential degradation procedure for MB dye molecules in an aqueous environment was proposed. This study presents an innovative photocatalyst for the water purification and decontaminate of dye molecules and other water pollutants in contaminated wastewater.

1. INTRODUCTION:

Dyes are unpleasant poisons due to the negative effects associated with oral consumption or inhalation, leading to ocular and dermal issues [1,2]. Excessive exposure to colored pollutants endangers us with respiratory, cardiovascular, central nervous system, and neurocognitive disorders, in addition to leukemia and autoimmune diseases [3-4]. Color is the principal contaminant present, often in minimal quantities. This occurs because colors inhibit the correct reoxygenation of water. Dye is a challenging material to eliminate because of its intricate makeup and synthetic origins. Water is vital for sustaining ecological and enhancing quality of life; therefore, it must be controlled before being released into water bodies [5-7]. Certain physical, chemical, or biological changes adversely affect water quality, rendering it hazardous for direct use [8]. Numerous enterprises release untreated effluents into freshwater sources, with colors identified as significant water contaminants. A variety of physical, chemical, and biological methods are employed to treat this aqueous sludge [9,10]. Photocatalysis might be considered one of the most vital methods as it does not generate any secondary pollutants.

Chitosan (CS), an environmentally benign material with low production costs, has garnered considerable acceptance in various domains such as water treatment, food packaging, tissue engineering, sensor fabrication, and pharmaceutical delivery due to its reliable biocompatibility, biodegradability, low immunogenicity, elevated permeability, antibacterial properties, advantageous optical attributes, and superior film-forming ability [11-12]. The highly delocalized, polarized, and electron-rich π bonds that constitute the alternating single and double bonds in a conjugated carbon chain enhance the optical characteristics of CS. The lone-pair electrons that the nitrogen and hydrogen atoms in the amine and hydroxyl functional groups of CS possess are crucial for a polymer electrode system because they enable coordinated interactions with charged particles. [13]. The unceasing interactions between charge carriers and the attainable functional groups will facilitate the transit of polymer chain segments, resulting in conductive behavior of the polymer. Nevertheless, it is low [14]; the cause of the diminished conductivity is attributed to the tightly bonded hydrogen atom in CS. A considerable amount of solution, either water or electrolyte, can be retained and absorbed by the CS membranes. This attribute enables CS membranes to exhibit ionic mobility, which is crucial for electrochemical investigations [15]. A notable drawback of utilizing CS as an electrode is its limited conductivity. An additional drawback is that extended use may

result in organic liquid solvent leaks from the CS electrode, hence diminishing ionic conductivity [16]. A further drawback is its inadequate chemical resistance, as the amino and hydroxyl groups in CS are essential for enhancing electrode resistance by obstructing anions and large molecules [17].

The aforementioned difficulties might be resolved by effectively spreading inorganic fillers of nano or submicron dimensions throughout the polymer. It has been shown that fillers can substantially influence the properties of polymer electrodes. Inorganic fillers may be used into materials to inhibit polymer crystallization, hence facilitating ion mobility during the morphological phase and augmenting electrochemical stability at the interfacial boundary [18]. Transition-metal dichalcogenides (TMDs), including MoS_2, SnS_2, and WS_2, have garnered significant attention for their exceptional mechanical and electrical properties, elevated spin-orbit coupling, altered bandgap, atomic-scale thickness, catalytic characteristics, charge storage capabilities, and other notable attributes.

This study initially developed a composite catalytic system of CS. A photocatalyst composed of MoS_2@CS spheres with a high specific surface area was synthesized utilizing straightforward hydrothermal and in situ techniques, without the application of templates. The synthesized photocatalysts were utilized for the degradation of MB. The produced samples were characterized using various techniques. This study examined the synthesis and photocatalytic characteristics of the MoS_2 and CS core-shell structure, offering a novel approach for the development of photocatalysts for dye wastewater remediation.

2. Experimental:

2.1 Materials

The creation of the photocatalyst entails the use of essential components, specifically chitosan, sodium molybdate dihydrate, and methylene blue (MB), obtained from Sigma Aldrich. Hydrochloric acid and sodium hydroxide were utilized for pH adjustment. All solutions were prepared utilizing deionized water.

2.2 Synthesis of MoS_2

The MoS_2 nanoflower was produced via the hydrothermal technique. Sodium molybdate dihydrate ($Na_2MoO_4{\cdot}2H2O$) was necessary as the molybdenum (Mo) source, together with (CH_4N_2S). Sodium molybdate dihydrate and thiourea were first suspend in 150 ml of deionized water, and then subjected to vigorous stirring, resulting in a translucent solution. The solution was subsequently placed in a 200 mL Teflon-lined autoclave and subjected to hydrothermal treatment for 20 h at 240 °C. The precipitate was subjected to centrifugation and subsequently washed with ethanol and deionized water. The resultant black powder was made to dry at 80 °C for 20 h to produce MoS_2 nanoflowers [19].

2.3 Preparation of nanocomposite

Solution casting was used to create the MoS_2@CS nanocomposite film, with MoS_2 concentrations ranging from 0.1 weight percent to 0.5 weight percent. One and a half grammes of CS were dissolved in a 1% acetic acid aqueous solution, and vigorous mechanical stirring was done at room temperature to create a base solution known as the CS solution. 3 mL of diluted CS solution, 15 mg of MoS_2 and fifteen millilitres of deionised water were combined to create a dopant solution of MoS_2. A small amount of CS and three millilitres of 1% acetic acid were used to create this diluted CS solution. The aggregation of MoS_2 is prevalent and typically settles near the bottom of the beaker [20]. Therefore, the dopant solution was mixed with a diluted chitosan solution to ensure the best possible dispersibility and stability. As a surfactant, CS provides MoS_2 with hydroxyl, carboxyl, and amino groups to coat its surface. This promotes homogeneous dispersion by reducing the chance of MoS_2 aggregation. Subsequently, to make the film, the requisite volume of dopant solution was introduced into the base solution utilising a pipette and agitated with a magnetic stirrer at 45 °C. 5 mL of glycerol were included into the entire solution to enhance its viscosity. The diluted CS solution is of such little quantity that it does not influence the overall composite concentration. Subsequently, as soon as the solution attained sufficient viscosity to create a film, it was transferred into a Petri dish and allowed to dry at ambient temperature until the film was established. The film was meticulously removed from the Petri plate once adequately dried and kept for future characteriszation [21].

3. RESULTS AND DISCUSSION:

3.1 XRD studies

The results of X-ray diffraction (XRD) analysis of the materials' crystal structures are shown in Fig. 1. Cai et al. (2017) found that the characteristic crystalline structure of CS is represented by the diffraction peaks at 2θ = 10.7° and 19.9°. The diffraction peaks at 14.5°, 33.0°, 39.8°, and 58.4° are associated with the MoS2 crystalline planes (002), (100), (103), and (110) (JCPDS 65-1951). The incorporation of CS considerably reduces the strength of its diffraction peaks, and MoS_2 diffraction peaks similarly decrease. This phenomenon validates the effective functionalisation of CS and the chemical reaction between MoS_2 and CS while synthesis [22-23].

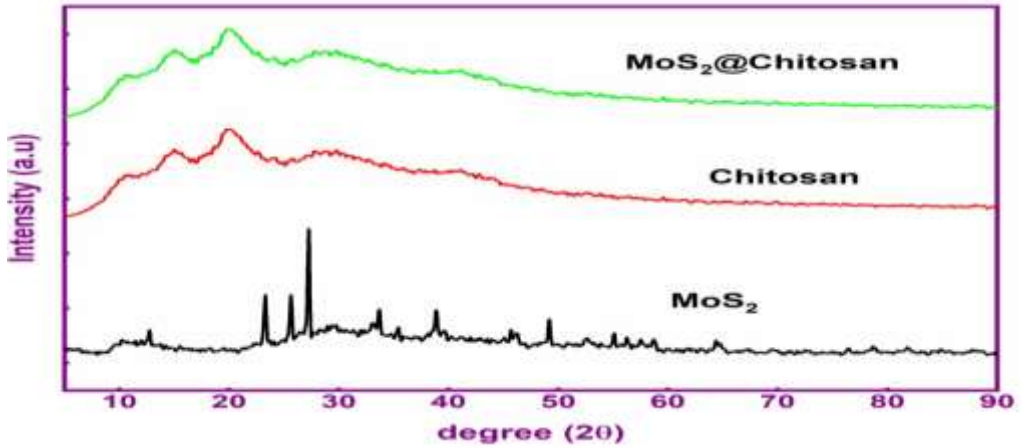

Fig.1 XRD of MoS_2, CS and MoS_2@CS

3.2 Morphology:

SEM was used to investigate the surface morphology of CS, MoS_2 nanoflower, and MoS_2@CS nanocomposite film; the resulting images are shown in Fig. 2(a)-(c). Figure 2(a) displays the SEM images of the CS film, revealing a smooth and uniform surface free of any pores throughout the film. Figure 2(b) illustrates the SEM image of MoS_2 particles exhibiting several nanoscale petals. The petals are irregularly linked and thickly grouped around a central point, like a spherical flower. The discovered porous architecture of MoS_2 nanoflowers substantially influences the electrochemical activity of the nanocomposites. Figure 2(c) depicts the SEM image of MoS_2@CS, validating the presence of MoS_2 nanoparticles by revealing petals encased within CS. MoS_2@CS nanocomposite films reveal remarkably a lot of prominent pores, due to the creation of MoS_2 nanoparticles on the surface. The porous structure enhances the influx of ion particles to the surface of the active materials. The inclusion of MoS_2 markedly improves the surface roughness of the films, hence increasing the surface area [24]. The raise in surface area will expose more active sites, hence improving electrochemical performance.

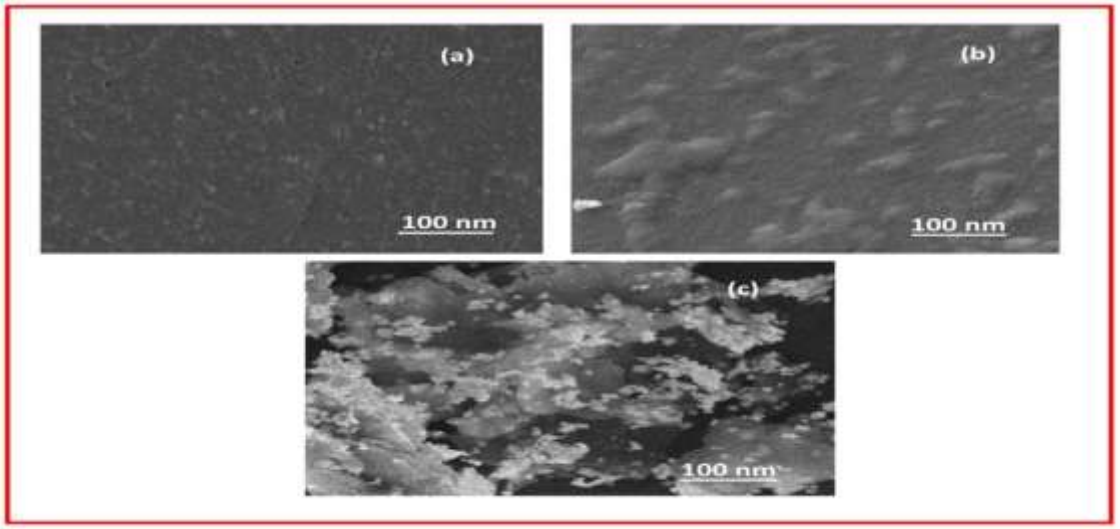

Fig.2 SEM images (a) CS (b) MoS_2 and (c) MoS_2@CS

3.3 Optical Properties

International Journal of Environmental Sciences
ISSN: 2229-7359
Vol. 11 No. 21s, 2025
https://theaspd.com/index.php

The optical characteristics of the synthesised CS and MoS_2 composite catalysts were examined using UV–Vis DRS absorption spectroscopy, as shown in Fig. 3a. In comparison to the MoS_2@CS The absorption edge of the synthesised CS and MoS_2@CS composite heterojunction exhibits a significant redshift and enhanced absorption in the visible-light spectrum, including a substantial percentage of both the UV and visible-light ranges. Simultaneously, the absorption intensity increases with the proportionate increase in MoS_2 content. Consequently, the optical bandgap energies (Eg) were derived using the Kubelka-Munk plots, specifically plotting $(\alpha hv)^{1/2}$ against the photon energy (hv) as illustrated in Fig. 3b; here, h, α, and v represent the Planck constant, diffuse absorption coefficient, and light frequency, respectively. The optical Eg values are determined to be 3.1 eV for the as-synthesized CS sample and 3.2 eV for the MoS2@CS composite sample. The alterations in the optical absorption spectrum may be attributed to the reduced coupling length and the associated quantum confinement effects [25]. Furthermore, the diminished optical bandgap of the MoS_2@CS composite heterojunction may enhance visible-light absorption efficiency due to the narrow optical Eg characteristics of MoS_2, potentially benefiting the absorption of additional photons to produce more photo-excited charge carriers by improving separation efficiency [26]. Consequently, it can significantly enhance the photocatalytic degradation of dyes.

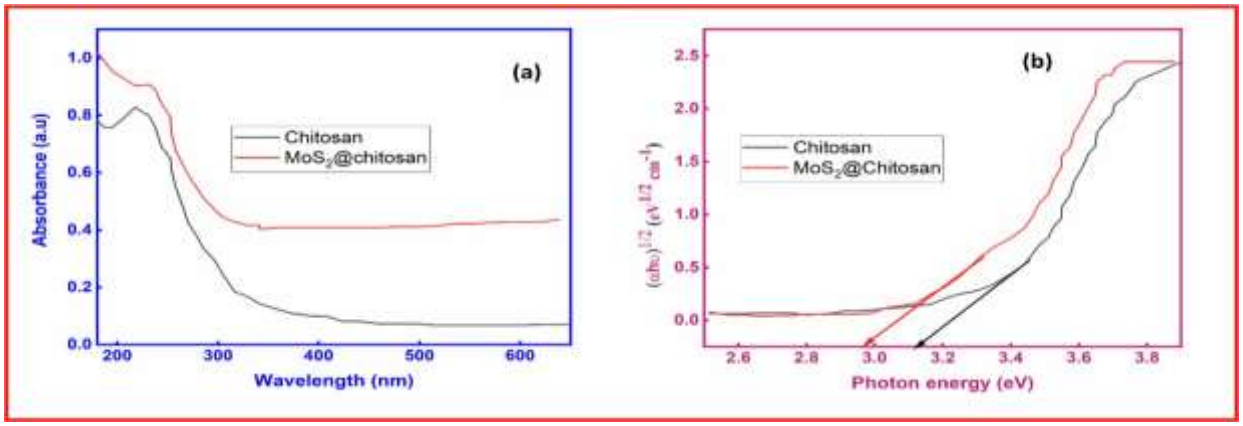

Fig 3 (a) UV-Vis of CS and MoS_2@CS (b) Tauc's plot of CS and MoS_2@CS

The photo-degradation efficacy was investigated using standard RhB aqueous organic contaminants under light exposure to evaluate the photo-degradation capabilities of the synthesised catalytic sample [27]. Figure 4a illustrates the photocatalytic degradation efficacy of the MoS_2@CS heterojunction sample on the degrading of the organic dye methylene blue (MB). Figure 6a illustrates that the absorbance of the MB aqueous dye solutions diminishes consistently with prolonged light exposure, indicating that the dyes are gradually destroyed. In the absence of a catalyst, over 3% of aqueous MB dyes were destroyed (Fig. 4b), indicating that the self-decomposition of the dyes is insignificant [28]. The unblemished CS composite film exhibited minimal disintegration in the absorption of aqueous MB (30.5%) dye solution during 90 minutes of light exposure.

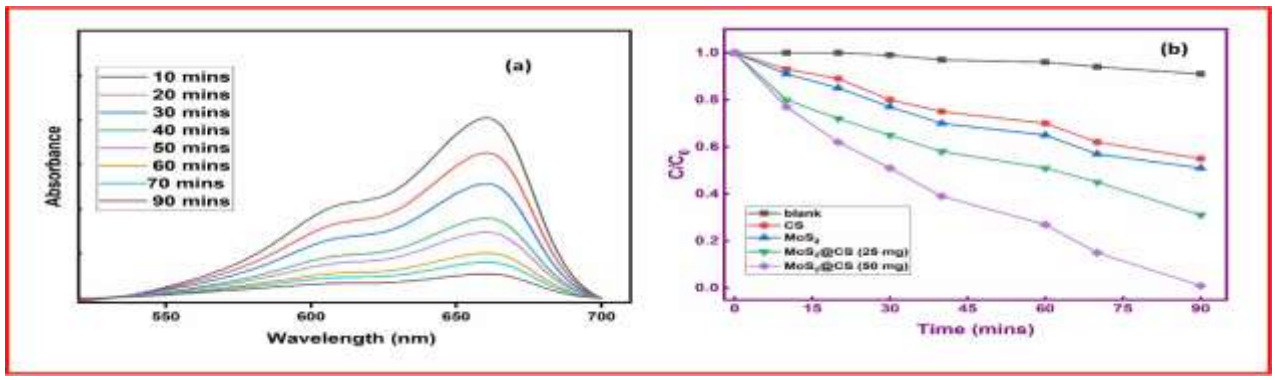

Fig 4 (a) UV absorption spectrum of MB degradation with MoS_2@CS (b) Photocatalytic degradation of MB with different photocatalyst

CONCLUSION:

In summary, the CS and MoS_2 hybrid nanocomposite (CS@MoS2) exhibited outstanding photocatalytic efficacy for the degrading of MB dye in aqueous solutions when exposed to visible light. The production of this hybrid material mitigated the constraints of MoS_2 by improving dye degradation efficiency. Thorough characterisation via XRD, SEM, UV-visible, and PL spectroscopy validated the structural integrity and photocatalytic efficacy of the MoS_2@CS nanocomposite. Enhancing factors, including irradiation duration, pH, dose, and beginning dye concentration, resulted in a remarkable 95% breakdown efficiency of MB within 90 minutes at pH 8, utilising only 50 mg of the catalyst. The limited band gap of the MoS_2@CS composite was essential in promoting the degradation of MB, underscoring its applicability in environmental contexts. This study not only presents a method for eliminating toxic dyes from industrial effluent but also elucidates the breakdown mechanism of MB under photocatalytic conditions. The MoS_2@CS hybrid nanocomposite demonstrates considerable potential as a sustainable and efficient photocatalyst for water purification, aiding in the detoxification of aquatic ecosystems from industrial pollutants.

REFERENCES:

1. S. Gautam, H. Agrawal, M. Thakur, A. Akbari, H. Sharda, R. Kaur, M. Amini, Metal oxides and metal organic frameworks for the photocatalytic degradation: a review, J. Environ. Chem. Eng. 8 (2020) 103726,
2. C. Xu, P. Ravi Anusuyadevi, C. Aymonier, R. Luque, S. Marre, Nanostructured materials for photocatalysis, Chem. Soc. Rev. 48 (2019) 3868–3902,
3. Raja, A. Antony Christian, et al. "Fabrication of Gd2O3-Loaded nitrogen-rich C3N5@ PANI hybrid nanocomposites: Unlocking efficient photocatalysis for long-Term organic dye degradation in wastewater treatment." Physica B: Condensed Matter 698 (2025): 416758.
4. Valli, KS Pushpa, et al. "Evaluating the photocatalytic efficiency of polypyrrole-enhanced Bi_2WO_6/g-C_3N_5 nanocomposites for effective organic pollutant degradation." Next Materials 8 (2025): 100557.
5. Y. Li, Z. Li, Y. Xia, H. Li, J. Shi, A. Zhang, H. Huo, S. Tan, L. Gao, Fabrication of ternary AgBr/BiPO4/g-C3N4 heterostructure with dual Z-scheme and its visible light photocatalytic activity for Reactive Blue 19, Environ. Res. 192 (2021) 110260,
6. Shanthini, K., et al. "Dynamic Trio: CuWO4@ C3N5/Polypyrrole nanocomposites Combat Chlorpyrifos and Rhodamine B in waste water." Surfaces and Interfaces 51 (2024): 104673.
7. J. Yan, Z. Song, X. Wang, Y. Xu, W. Pu, H. Xu, S. Yuan, H. Li, Enhanced photocatalytic activity of ternary Ag3PO4/GO/g-C3N4 photocatalysts for Rhodamine B degradation under visible light radiation, Appl. Surf. Sci. 466 (2019) 70–77.
8. Hongbin Yu, Danyang Wang, Bin Zhao, Ying Lu, Xinhong Wang, Suiyi Zhu, Weichao Qin, Mingxin Huo, "Enhanced photocatalytic degradation of tetracycline under visible light by using a ternary photocatalyst of Ag_3PO_4/AgBr/g-C_3N_4 with dual Z-scheme heterojunction", Separation and Purification Technology, Vol. 237, 2020, 116365,
9. Xiarong Zheng, Yuanqiong Liu, Xiaobin Liu, Qingbiao Li, Yanmei Zheng, "A novel PVDF-TiO_2@g-C_3N_4 composite electrospun fiber for efficient photocatalytic degradation of tetracycline under visible light irradiation", Ecotoxicology and Environmental Safety, Vol. 210, 2021, 111866
10. Deli Jiang, Wanxia Ma, Peng Xiao, Leqiang Shao, Di Li, Min Chen, "Enhanced photocatalytic activity of graphitic carbon nitride/carbon nanotube/Bi_2WO_6 ternary Z-scheme heterojunction with carbon nanotube as efficient electron mediator", Journal of Colloid and Interface Science, Vol. 512, 15 2018, Pages 693-700.
11. Wei Wang, Jiaojiao Fang, Shaofeng Shao, Min Lai, Chunhua Lu, Compact and uniform TiO_2@g-C_3N_4 core-shell quantum heterojunction for photocatalytic degradation of tetracycline antibiotics, Applied Catalysis B: Environmental, Volume 217, 2017, Pages 57-64.
12. Rahman, Tanzim Ur, et al. "Sustainable toxic dye removal and degradation from wastewater using novel chitosan-modified TiO2 and ZnO nanocomposites." Journal of Molecular Liquids 388 (2023): 122764.
13. Anirudhan, Thayyath S., F. Shainy, and J. Christa. "Synthesis and characterization of polyacrylic acid-grafted-carboxylic graphene/titanium nanotube composite for the effective removal of enrofloxacin from aqueous solutions: Adsorption and photocatalytic degradation studies." Journal of hazardous materials 324 (2017): 117-130.
14. Gupta, Vinod Kumar, et al. "$CoFe_2O4$@ TiO_2 decorated reduced graphene oxide nanocomposite for photocatalytic degradation of chlorpyrifos." Journal of Molecular Liquids 208 (2015): 122-129.
15. Mondal, Prasenjit, C. B. Majumder, and Bikash Mohanty. "Laboratory based approaches for arsenic remediation from contaminated water: recent developments." Journal of Hazardous materials 137.1 (2006): 464-479.
16. Nawaz, Arif, et al. "Fabrication and characterization of new ternary ferrites-chitosan nanocomposite for solar-light driven photocatalytic degradation of a model textile dye." Environmental Technology & Innovation 20 (2020): 101079.
17. Manubolu, M., K. Pathakoti, and J. Leszczynski. "Recent advances in chitosan-based nanocomposites for dye removal: a review." International Journal of Environmental Science and Technology 21.4 (2024): 4685-4704.
18. Alimard, Paransa. "Fabrication and kinetic study of Nd-Ce doped Fe3O4-chitosan nanocomposite as catalyst in Fenton dye degradation." Polyhedron 171 (2019): 98-107.
19. Feng, Wei, et al. "Flower-like PEGylated MoS2 nanoflakes for near-infrared photothermal cancer therapy." Scientific reports 5.1 (2015): 17422.

20. Mohammed, Mustafa KA, et al. "Facile synthesis of chitosan-MoS2 over reduced graphene oxide to improve photocatalytic degradation of methylene blue." Journal of Sol-Gel Science and Technology (2024): 1-11.
21. Sirajudheen, P., et al. "Mechanistic view of MoS2 confined chitosan-polyaniline hybrid composite for the photo-oxidation of cationic dyes." International Journal of Biological Macromolecules 249 (2023): 126008.
22. Nikitha, M., S. SD Elanchezhiyan, and S. Meenakshi. "Photodegradation of rhodamine-B in aqueous environment using visible-active g-C3N4@ CS-MoS2 nanocomposite." Environmental research 238 (2023): 117032.
23. Liu, Kai, et al. "Enhanced degradation of azo dyes wastewater by S-scheme heterojunctions photocatalyst g-C3N4/MoS2 intimately coupled Rhodopseudomonas palustris with chitosan modified polyurethane sponge carrier." International Journal of Hydrogen Energy 48.58 (2023): 22319-22333.
24. Cao, Wenbo, et al. "Photodynamic chitosan functionalized MoS2 nanocomposite with enhanced and broad-spectrum antibacterial activity." Carbohydrate Polymers 277 (2022): 118808.
25. Islam, Muhammad Rakibul, Eashika Mahmud, and Rabeya Binta Alam. "MoS2 nanoflower decorated bio-derived chitosan nanocomposites for sustainable energy storage: Structural, optical and electrochemical studies." Heliyon 10.3 (2024).
26. Al Momani, Delal E., Fathima Arshad, and Linda Zou. "Chitosan/MoS2/GO membrane for catalytic degradation of organic contaminants." Environmental Technology & Innovation 32 (2023): 103410.
27. Mohammed, Mustafa KA, et al. "Facile synthesis of chitosan-MoS2 over reduced graphene oxide to improve photocatalytic degradation of methylene blue." Journal of Sol-Gel Science and Technology (2024): 1-11.
28. Sirajudheen, Palliyalil, et al. "Fabrication of MoS2 restrained magnetic chitosan polysaccharide composite for the photocatalytic degradation of organic dyes." Carbohydrate Polymers 335 (2024): 122071.